Small-Field Galvanomagnetic Tensor of Bismuth at 4.2°K*†

R. N. ZITTER‡
Department of Physics and Institute for the Study of Metals, University of Chicago, Chicago, Illinois
(Received March 20, 1962)

Values of carrier concentrations and mobilities in large monocrystalline samples of bismuth at 4.2°K have been derived from measurements of all the galvanomagnetic tensor components through second order in magnetic field. Fields of the order of one gauss and less are required, and a superconducting chopper amplifier detects the minute voltages involved. The electron concentration is found to be 2.5×10^{17} cm^{-3}, and the concentration of "light" holes is very nearly the same. When compared with cyclotron resonance and de Haas-van Alphen experiments, the results are consistent with a three-ellipsoid model for electrons and a single ellipsoid for "light" holes. There is no indication of the presence of "heavy" holes in a concentration comparable to the other carriers. Electron and "light"-hole relaxation times are isotropic to within a factor of 2; for electrons, $\tau\doteq2\times10^{-10}$ sec, and for holes, $\tau\doteq5\times10^{-10}$ sec. Some of the effects of temperature and of larger magnetic fields are discussed.

I. INTRODUCTION

INVESTIGATIONS of the band structure of bismuth show puzzling anomalies. Electron masses obtained from a variety of techniques are in good agreement, but the question of whether three or six ellipsoids represent the conduction band apparently has experimental support on both sides.[1] The multiplicity of hole ellipsoids is also under debate, as well as the possible existence of a third set of carriers (a heavy-hole band) which seems necessary to explain specific heat data.

A complete measurement of the small-field galvanomagnetic tensor components at low temperatures hopefully can help reduce this confusion. The experiment is traditionally one of the most direct methods of obtaining carrier concentrations and their mobilities; from these, deductions can be made about ellipsoid multiplicities, relaxation times, and the existence of a third set of carriers.

Previous galvanomagnetic studies on bismuth include the measurements of Abeles and Meiboom[2] at 80 and 300°K and those of Okada[3] from 113 to 318°K. For temperatures below 80°K, published small-field data are fragmentary. Actually, these are the desirable temperatures for study because the bands are highly degenerate; then in the theory it is not necessary to consider the dependence of relaxation time on energy but only the value at the Fermi energy. As a result, there will be no significant difference between drift, Hall, and magnetoresistance mobilities, provided that τ is not highly anisotropic over each energy ellipsoid.

Helium temperature measurements are difficult due to the combination of very large carrier mobilities and long mean free paths. At 4.2°K, magnetic fields not exceeding the order of one gauss are required to satisfy the small-field condition $\omega\tau=\mu H/c\ll1$. Stray fields, including terrestrial magnetism, must be canceled and sample currents limited to avoid generating excessive self-fields. At the same time, sample thicknesses of at least 0.5 cm are required to avoid serious size effects.[4] Under these restrictions, magnetoresistance and Hall voltages are in the range 10^{-8} to 10^{-10} V. At these temperatures, however, a superconducting chopper amplifier may be used [noise$=10^{-11}$ V/(cps)$^{1/2}$] in place of the usual galvanometer, and direct-current measurements can be made in the normal manner.

II. THEORY

The theory may be divided into two parts: the first is phenomenological, while in the second, details of the transport process based on the Boltzmann equation and the shape of the Fermi surface are introduced.

The phenomenological theory begins with a generalized Ohm's law for a crystalline solid:

$$E_i=\sum_j \rho_{ij}(\mathbf{H})J_j, \tag{1}$$

relating components of the electric field and the current density through a resistivity tensor whose components are functions of the magnetic field. For sufficiently small fields, the expansion

$$\rho_{ij}(\mathbf{H})=\rho_{ij}{}^0+\rho_{ij,k}H_k+\rho_{ij,kl}H_kH_l+\cdots \tag{2}$$

is assumed valid, and the only restrictions on (2) are the requirements of crystal symmetry and the Onsager (time-reversal symmetry) relations. This means that a number of components in Eq. (2) may vanish, while others will be functionally related. The necessary group theoretic analysis has already been carried out for the $3\bar{m}$ symmetry of bismuth by Okada[5] and by Juretschke[6];

* Submitted as a thesis in partial fulfillment of the requirements for the degree of Doctor of Philosophy at the University of Chicago.

† The work was supported in part by a grant from the National Science Foundation to the University of Chicago for research on the solid-state properties of bismuth, antimony, and arsenic.

‡ Now with Bell Telephone Laboratories, Murray Hill, New Jersey.

[1] W. A. Harrison and M. B. Webb, Editors, *The Fermi Surface* (John Wiley & Sons, Inc., New York, 1960). This book provides a comprehensive view of the current state of knowledge of the Fermi surface in bismuth.

[2] B. Abeles and S. Meiboom, Phys. Rev. **101**, 544 (1956).

[3] T. Okada, J. Phys. Soc. Japan **12**, 1327 (1957).

[4] A. N. Friedman and S. H. Koenig, IBM J. Research Develop. 4, 158 (1960).

[5] T. Okada, J. Phys. Soc. Japan **11**, 89 (1956).

[6] H. J. Juretschke, Acta Cryst. **8**, 716 (1955).

it is found that the tensors ρ_{ij}^0 and $\rho_{ij,k}$ each have only two independent components while $\rho_{ij,kl}$ has eight.

Therefore, there is a total of 12 independent resistivity tensor components to second order in magnetic field. It may be noted that due to the sign convention of Eq. (2), the $\rho_{ij,k}$ are the negatives of the usual Hall coefficients. The notation being used here is that of Okada.

In analogy to (1) and (2), one can write

$$J_i=\sum_j \sigma_{ij}(\mathbf{H})E_j, \tag{3}$$

$$\sigma_{ij}(\mathbf{H})=\sigma_{ij}^0-\sigma_{ij,k}H_k-\sigma_{ij,kl}H_kH_l-\cdots, \tag{4}$$

where the conductivity tensor $\sigma_{ij}(\mathbf{H})$ is the mathematical inverse of $\rho_{ij}(\mathbf{H})$ and has all the same symmetry properties. The relationships between the elements of Eqs. (2) and (4) can be found in the papers of Okada and Juretschke.

Experimentally, Eq. (1) is more convenient than Eq. (3) because current and magnetic field directions are easily controlled, while this is not the case for electric field. In the theory, however, conductivities are computed first, so the best procedure is to convert these to ρ's for comparison with the data. The reverse process of calculating conductivities from the data only compounds experimental errors.

The theoretical computation of the conductivity tensor components begins by considering the transport properties of a single energy ellipsoid. Abeles and Meiboom[2] pointed out that if a relaxation time exists, the transport relation,

$$\mathbf{J}=\boldsymbol{\sigma}^0\cdot[\mathbf{E}+(nec)^{-1}\mathbf{J}\times\mathbf{H}],$$

follows from the Boltzmann equation when the relaxation time is isotropic (a function of energy only). Here n is the carrier concentration of the ellipsoid, and the zero-field conductivity tensor $\boldsymbol{\sigma}^0$ can be written

$$\boldsymbol{\sigma}^0=ne\mathfrak{y}=ne^2\tau\mathbf{m}^{*-1},$$

where $\mathfrak{y}$ is the mobility tensor, τ is the relaxation time, and $\mathbf{m}^{*-1}$ is the reciprocal effective-mass tensor. The other symbols have the meanings given earlier. The above relation can be solved explicitly for $\mathbf{J}$ and the result has the form of Eq. (3); a power series expansion in magnetic field, as in Eq. (4), gives the small-field conductivity tensors for the ellipsoid.

The restriction of an isotropic relaxation time may be relaxed somewhat if the formalism of Herring and Vogt[7] is adopted. In this approach, the relaxation time is a tensor:

$$\mathfrak{y}=e\boldsymbol{\tau}\cdot\mathbf{m}^{*-1}, \tag{5}$$

and the components of $\boldsymbol{\tau}$ are each separate functions of the energy, i.e., each component is dependent on energy only. A scalar τ dependent on energy only corresponds to the special case of $\boldsymbol{\tau}$ having identical components. Herring and Vogt also assumed that the principal axes of $\boldsymbol{\tau}$ and $\mathbf{m}^{*-1}$ are the same, but this is actually not necessary for the results to follow.

The small-field conductivity tensors were obtained by Herring and Vogt using classical statistics. The conversion to the case of a strongly degenerate Fermi distribution is not difficult, and when the results are expressed in terms of mobilities according to (5), one finds them to be identical with the earlier results of Abeles and Meiboom. This is not surprising, since essentially the only change has been to replace $\tau\mathbf{m}^{*-1}$ in the Boltzmann equation by $\boldsymbol{\tau}\cdot\mathbf{m}^{*-1}$ and in each case the product has been labeled by the same symbol $\mathfrak{y}$. (Different results are expected for nondegenerate statistics, when averages over energy are involved.)

Herring and Vogt have shown also that for a number of calculable cases, their approach is a good approximation provided the "anisotropy" or difference between the components of $\boldsymbol{\tau}$ is not too great; component ratios of 2 certainly give good results. Accordingly, there are some grounds for confidence if an analysis of data by means of this model gives relaxation time components which are not too different.

As a final step in the theoretical calculations, the conductivities of a single ellipsoid must be summed over all appropriate valleys. For bismuth, the Fermi surface currently proposed[1] consists, briefly, of three sets of ellipsoids for electrons in threefold rotational symmetry about the trigonal axis and tilted slightly out of the trigonal plane, with centers on the binary axes; holes are represented by a set of ellipsoids of revolution along the trigonal axis. The calculation for electrons involves rotations of an ellipsoid to various directions in momentum space to determine the effect of the galvanomagnetic components.

The total conductivity tensor is found to have the following components (in mks units, to avoid powers of the velocity of light):

$$\begin{aligned}
\sigma_{11}^0/e&=\tfrac{1}{2}N(\mu_1+\mu_2)+P\nu_1,\\
\sigma_{33}^0/e&=N\mu_3+P\nu_3,\\
\sigma_{23,1}/e&=\tfrac{1}{2}N(\mu_1\mu_3+\mu_2\mu_3-\mu_4^2)-P\nu_1\nu_3,\\
\sigma_{12,3}/e&=N\mu_1\mu_2-P\nu_1^2,\\
\sigma_{11,11}/e&=\tfrac{1}{8}N[(\mu_1-\mu_2)^2\mu_3+(5\mu_1-\mu_2)\mu_4^2],\\
\sigma_{11,22}/e&=\tfrac{1}{8}N[(3\mu_1^2+3\mu_2^2+2\mu_1\mu_2)\mu_3-(\mu_1+3\mu_2)\mu_4^2]\\
&\qquad +P\nu_1^2\nu_3,\\
\sigma_{11,33}/e&=\tfrac{1}{2}N\mu_1\mu_2(\mu_1+\mu_2)+P\nu_1^3,\\
\sigma_{33,11}/e&=\tfrac{1}{2}N[(\mu_1+\mu_2)\mu_3^2-\mu_3\mu_4^2]+P\nu_1\nu_3^2,\\
\sigma_{33,33}/e&=N\mu_1\mu_4^2,\\
\sigma_{11,23}/e&=\tfrac{1}{4}N\mu_1(\mu_1-\mu_2)\mu_4,\\
\sigma_{23,11}/e&=\tfrac{1}{4}N[(\mu_1-\mu_2)\mu_3\mu_4+\mu_4^3],\\
-\sigma_{23,23}/e&=\tfrac{1}{2}N\mu_1\mu_2\mu_3+\tfrac{1}{2}P\nu_1^2\nu_3.
\end{aligned} \tag{6}$$

Here, N and P are the total carrier concentrations and μ_i and ν_i are the components of the electron and hole

[7] C. Herring and E. Vogt, Phys. Rev. **101**, 944 (1956).

mobility tensors in the crystal axes coordinate system:

$$\mathfrak{y}=\begin{pmatrix}\mu_1 & 0 & 0\\ 0 & \mu_2 & \mu_4\\ 0 & \mu_4 & \mu_3\end{pmatrix}, \tag{7}$$

$$\mathfrak{v}=\begin{pmatrix}\nu_1 & 0 & 0\\ 0 & \nu_1 & 0\\ 0 & 0 & \nu_3\end{pmatrix}. \tag{8}$$

The electron mobility tensor, Eq. (7), is simply the result of rotating (5) through the ellipsoid tilt angle, which can be expressed as

$$\tan 2\theta = 2\mu_4/(\mu_3-\mu_2). \tag{9}$$

All mobility components are taken positive, with the possible exception of μ_4, whose sign depends on the tilt angle.

N and P are integral multiples of the carrier concentrations per ellipsoid. Electrical neutrality is assumed here, but N and P will differ if a significant contribution comes from ionized impurities, or if there is a third set of carriers so heavy that they do not otherwise contribute to the conductivities in Eq. (6).

The equations (6) are essentially equivalent to those reported by Freedman and Juretschke[8] in their work on antimony, and several important features should be noted.

First of all, $\sigma_{23,23}$ is definitely negative. This is not predicted by phenomenological theory, so it must come from assumptions made about the shape of the Fermi surface and the "geometry" of τ, i.e., the dependence of relaxation time on momentum. It happens that the corresponding component $\rho_{23,23}$ has no sign restriction so an important test of the model is to compute $\sigma_{23,23}$ from the data and then inspect its sign.

Other tests of the model come from the fact that the relations (6) are not all independent. At first glance, it would seem simply that Eq. (6) is a set of 12 equations in eight unknowns (four electron and two hole mobilities, and N and P) so there should be four relationships between the σ's of Eq. (6). Two of these relations, however, are quite unique. They are

$$\sigma_{11,22}+2\sigma_{33,33}=3\sigma_{11,11}+2(-\sigma_{23,23}), \tag{10}$$

$$\sigma_{11,11}+(4\sigma_{23,1}/\sigma_{12,3})\sigma_{11,33}+(4\sigma_{11}^{0}/\sigma_{33}^{0})\sigma_{33,11}$$
$$=3\sigma_{11,22}+[2+(8\sigma_{11}^{0}/\sigma_{33}^{0})(\sigma_{23,1}/\sigma_{12,3})](-\sigma_{23,23}), \tag{11}$$

and their remarkable property is that they have very little to do with the number of unknowns. It can be verified that they hold not only in the present case but also when there are no holes, or two sets of holes, or even if there were 10 sets of carriers, in which case there would be more unknowns than equations.

Since phenomenological theory allows 12 independent tensor components by crystal and time reversal symmetry, Eqs. (10) and (11) must come from the model. The additional symmetry implied by the relations is puzzling, because the model of the conduction band (three sets of tilted ellipsoids) apparently has just the crystal symmetry and no more. The author is not aware of any theoretical study of this point. From an experimental point of view, one would like to know if Eqs. (10) and (11) are all the relations there are, or if there are more. A relation of similar character for a cubic crystal has been investigated experimentally in germanium.[9]

The two remaining relations appropriate to Eq. (6) have been found, but they are quite complicated and essentially worthless for experimental application. In fact, a complete algebraic solution of (6) was discovered and then discarded, because it involved differences of quantities of the same order of magnitude.

The procedure, then, is to choose a set of values for the unknowns giving a best fit to the data. For this purpose, expressions for the resistivity tensor components have been calculated from (6) and, due to their length, are given in the Appendix.

So far, the theory has ignored the effects due to the finite size of samples. A size effect which has received attention in the past is the surface scattering of charge carriers; in particular, the measurements of Friedman and Koenig[4] show that surface scattering in bismuth is specular rather than diffuse. However, there is another size effect to consider when both electrons and holes are present. As experience with semiconductors has shown, the Lorentz force of the applied magnetic field tends to bring about a "pileup" of charge carriers at some surface, with the result that within a diffusion length of the surface, carrier concentrations may deviate from their bulk values, the amount depending strongly on the surface recombination velocity. If the diffusion length is comparable to sample thickness and surface recombination is small, galvanomagnetic measurements will not reflect bulk properties.

In semimetals, recombination takes place with zero energy loss, representing the intervalley scattering between electron and hole ellipsoids. Instead of the "diffusion length" of semiconductors, it is more proper to speak of a "recombination scattering length," i.e., the mean free path for recombination. The fact that specular reflection is predominant at bismuth surfaces implies a low rate of surface recombination, and so it is important in the present measurements to have samples with thicknesses that are large compared to the recombination length, which in turn may be larger than the mean free path. As described in a later section, it was verified that the thickness used was much larger than either of these lengths.

III. EXPERIMENTAL DETAILS

Superconducting Chopper Amplifier

This device basically is the same as any dc amplifier which "chops" the input and then amplifies only the

[8] S. J. Freedman and H. J. Juretschke, Phys. Rev. **124**, 1379 (1961).

[9] C. Goldberg and W. Howard, Phys. Rev. **110**, 1035 (1958).

alternating component, but instead of interrupting the input current by moving contacts, the transition from superconducting to normally conducting states in a magnetic field is used. The normal resistance of a fine wire can be made very large compared to the resistance of the rest of the circuit and corresponds to an open circuit condition.

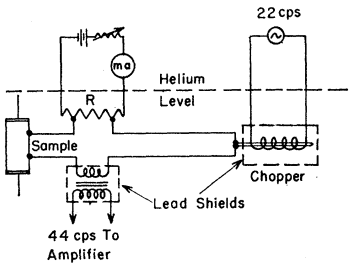

FIG. 1. The primary measuring circuit. The amplifier is used as a null detector and senses an unbalance between the voltage to be measured and that generated across a calibrated resistance R. For magnetoresistance experiments, the milliammeter is shunted to read only increments above a given value.

Compared to a noise level of about 10^{-9} V for the best mechanical chopper, the superconducting chopper has a noise of 10^{-11} V/(cps)$^{\frac{1}{2}}$ associated with the transition between states. Another advantage is that, with a small transformer in the helium bath, the signal leaving the cryostat is alternating and spurious thermoelectric sources in the leads (often as large as 10^{-7} V) are of no importance.

The first such amplifier was built by Templeton[10]; an improved version is due to de Vroomen and van Baarle[11] and served as a model for the present work, except that some changes were made to ease the load of required electronic hardware.

Figures 1 and 2 show the main features of the amplifier, used here as a null detector. Voltage in a sample of bismuth is bucked by passing a known current through a calibrated resistance, and the unbalance current is chopped and passes through the transformer primary winding.

The bucking resistor is simply a 1-in. length of No. 24 annealed copper wire. Repeated calibrations at regular intervals by a standard potentiometric technique showed little change in the resistance of $10^{-5}\,\Omega$ at 4.2°K.

The chopping element is a "noninductive" loop of 2-mil tantalum wire[12] inside a solenoid, and sinusoidal current through the solenoid causes transitions to the normally conducting state at both positive and negative peaks, so chopping occurs at twice the driving frequency. The critical magnetic field for tantalum is only about 50 G at 4.2°K but rises very rapidly with decreasing temperature. For this reason, indium (in the form of a thick film applied by soldering gun to a copper-beryllium wire) was substituted for measurements below 3.5°K. The lower critical field required meant reduced power consumption by the chopper solenoid and so reduced helium evaporation. Both chopper and transformer (a small toroid) are encased in separate superconducting shields, located far from the sample to avoid distorting the magnetic fields of the experiment.

If second harmonic distortion in the solenoid driving signal exceeds 0.1%, the pickup induced in the chopper element becomes large compared to the true signal. proper balancing of a push-pull driver stage meets the distortion requirement.

Another difficulty is the fact that superconducting circuits still have inductance which can represent a rather large impedance on the scale dealt with here. For example, the twisted pair of 2-mil niobium wire used to span the 15-in. distance between sample and chopper circuit had an inductive impedance of the order of $10^{-4}\,\Omega$ at the operating frequency of 44 cps. Inductances of this size lengthen the time constant of the measuring circuit, which can be decreased only by extra resistance and consequent loss of power. Extreme care, therefore, was taken to minimize all inductances and to avoid large area loops.

Sample Preparation

Large single crystals of conical shape were grown in a Pyrex funnel whose tip had been sealed. High-purity silicone oil protected the bismuth against oxidation and also prevented the melt from sticking to the walls; presumably this latter property is helpful also in minimizing the formation of crystal defects during growth.

The melt cooled slowly in a temperature gradient, crystallizing first at the tip. Complete solidification took about eight hours. The crystal slipped easily from the funnel when it was inverted, and after removal of the silicone oil with acetone, a strong nitric acid etch was used.

Single crystals were obtained only after the entire process was repeated four or five times. Apparently the bismuth initially contains included oxides which gradually are eliminated through successive crystallizations and etchings.

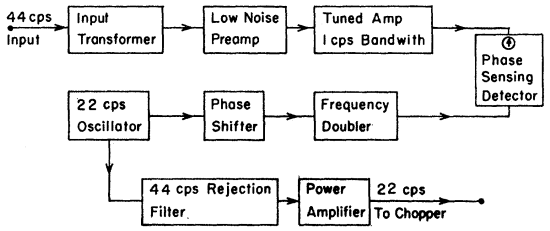

FIG. 2. Block diagram of the amplifier electronics outside of the helium bath.

Bismuth cleaves easily in a plane perpendicular to the trigonal axis. With this plane as reference, the crystal was mounted on a gonimeter and rotated to determine the binary axis by x-ray reflection.

[10] I. M. Templeton, J. Sci. Instr. **32**, 314 (1955).
[11] A. R. de Vroomen and C. van Baarle, Physica **23**, 785 (1957).
[12] Obtained from the Fansteel Metallurgical Corporation, North Chicago, Illinois.

Figure 3 shows the crystal and the samples derived from it; they were obtained directly in the shape shown by using a square copper tube mounted on an Isomet[13] spark cutting machine. This device cuts by spark erosion, and fairly sharp x-ray patterns can be obtained from a freshly cut surface without etching, indicating that damage extends into the sample to a depth of only some tenths of a micron. An acid string saw might be as gentle to a substance as fragile as bismuth but does not lend itself to the cutting of flat and parallel surfaces as required in the present experiment.

The samples measured 0.8×0.8 cm^2 in cross section and lengths ranged from 5 to 7 cm. Orientation with respect to crystal axes was within one degree in all cases.

Two crystals were grown, one from Cerro de Pasco bismuth of spectroscopic grade and one from commercially available zone refined ingots ("Tadanac" brand). Surprisingly, experimental results were almost identical for the two cases, and resistivities at 4.2°K were fairly low. In the spectroscopic grade, at least, it appears that impurities were removed during the repeated recrystallizations, by segregation during freezing, and then by oxidation and etching. At the same time, impurities may have been added to the zone-refined material (from the silicone oil, for example) so that both crystals ended up at a purity limit characteristic of the process. Alternatively, the limiting factor might be dislocations, introduced in crystal growth or sample cutting.

Sample Holder and Magnetic Fields

Samples were mounted on a Bakelite slab supported by thin-walled Monel tubes, as shown in Fig. 4. Alignment rings at the ends of the slab are a close fit to the inside of the Dewar, while the sample itself rests in a close-fitting groove machined in the slab. Other grooves accurately positioned the potential probes along the sample in the four-terminal arrangement commonly used in Hall and resistivity measurements. This procedure was successful in keeping the effects of probe misalignment to a small fraction of the quantities being measured.

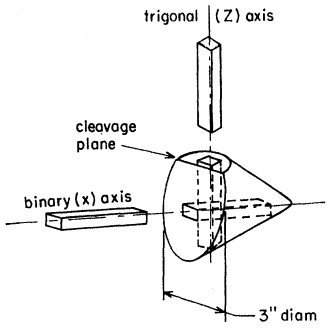

FIG. 3. Grown single crystal and the samples derived from it. The binary axis shown is 13° from the axis of the cone.

Resistivity probes were spaced 2 cm apart, roughly one third the length of the sample, to avoid end effects. Current connections were made through copper squares soldered to the ends of the sample, and only one end was fastened to the slab to prevent strain due to differences in thermal expansion. All soldering to or near the sample was done with bismuth-cadmium eutectic, a nonsuperconducting solder melting at 145°C. Care was taken never to overheat the solder because of the extreme toxicity of cadmium vapor.

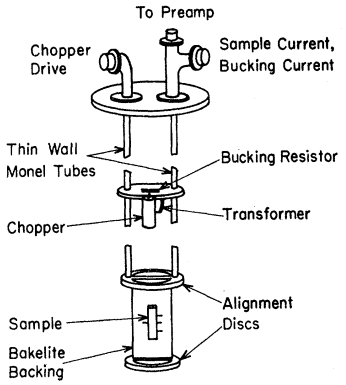

FIG. 4. Holder for the sample and parts of the superconducting chopper amplifier.

The chopper and first input transformer, encased in superconducting lead shields, were placed at a minimum distance of 12 in. from the sample to avoid distorting applied magnetic fields. The amount of distortion can be estimated by considering the effect of a superconducting sphere (perfectly diamagnetic) of roughly the same dimensions as the chopper and transformer, in a homogeneous magnetic field. From a distance, the sphere looks like an induced dipole, and at 12 in. from a 3-in. sphere the distortion is about 0.1% of the field at the sphere.

Superconducting wire leading from the chopper circuit to the sample was very thin (2-mil enameled niobium), again for reasons of field distortion.

Two sets of Helmholtz coils supplied fields perpendicular to each other in a horizontal plane; a third, vertical field was produced by an end-corrected solenoid[14] located in the nitrogen space between inner and outer Dewars. The three fields could give a resultant in any direction which was homogeneous to 0.1% over the volume of the sample; in addition, terrestrial magnetism and other stray fields were canceled by the coils so that not more than 10^{-2} G remained.

The alignment of the coils was adjusted until they were mutually perpendicular to within a small fraction of a degree, as determined by the minima of induced signals when alternating currents are sent through one of the coils. With flat pickup coils mounted on the Bakelite slab, the same technique could be used to fix the orientation of the samples with respect to the magnetic field.

[13] Purchased from Metals Research, Ltd., Cambridge, England.

[14] M. W. Garrett, J. Appl. Phys. 22, 1091 (1951).

IV. TENSOR COMPONENT MEASUREMENTS

Only two properly oriented samples are necessary to get all of the resistivity components. The quantities measured on a sample whose length is along the trigonal

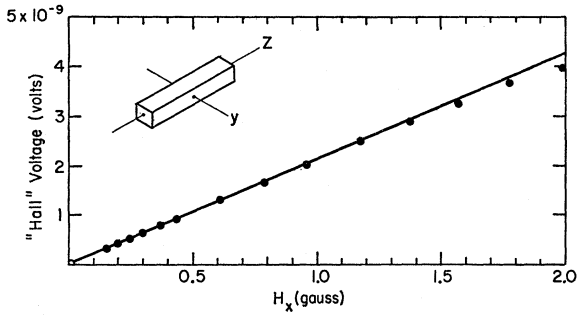

FIG. 5. Experimental plot for the Hall coefficient $\rho_{23,1}$, showing magnetic fields used and the voltages measured.

axis with sides parallel to the other crystal axes are

$$\rho_{33}=\rho_{33}^{0}+\rho_{33,11}(H_1^2+H_2^2)+\rho_{33,33}H_3^2, \quad (12)$$

$$\rho_{13}=-\rho_{23,1}H_2+2\rho_{23,11}H_1H_2+2\rho_{23,23}H_1H_3, \quad (13)$$

$$\rho_{23}=\rho_{23,1}H_1+\rho_{23,11}(H_1^2-H_2^2)+2\rho_{23,23}H_2H_3. \quad (14)$$

These represent one magnetoresistance and two Hall experiments (for the two pairs of sides), measuring all three components of electric field. When the sample is along a binary axis, the quantities are

$$\rho_{11}=\rho_{11}^{0}+\rho_{11,11}H_1^2+\rho_{11,22}H_2^2 +\rho_{11,33}H_3^2+2\rho_{11,23}H_2H_3, \quad (15)$$

$$\rho_{21}=-\rho_{12,3}H_3+(\rho_{11,11}-\rho_{11,22})H_1H_2+2\rho_{11,23}H_1H_3, \quad (16)$$

$$\rho_{31}=\rho_{23,1}H_2+2\rho_{23,11}H_1H_2+2\rho_{23,23}H_1H_3. \quad (17)$$

The second sample could also be taken along a bisectrix, but size effects are extreme in this direction.[4]

All 12 tensor components are seen here, some of them more than once. The redundancy is a valuable feature. Three of the components are measured in both samples, and this will show whether the two separate samples are in fact representative of the same bulk material. On the other hand, where a tensor component is determined by different experiments on the same sample, consistency means among other things that potential probes, sample geometry, and magnetic field are accurately aligned with the crystal axes.

In the present work, redundant values agreed within the relative experimental error, which ranged from 5% for $\rho_{23,1}$ to 15% for $\rho_{23,23}$. It was found that all of the alignment precautions mentioned in the previous section were necessary to achieve these results.

In all experiments, a number of magnetic field values were used in each tensor component determination, both for accuracy and to ensure that small field conditions applied, i.e., linearity with H for Hall terms and with H^2 for second-order terms. Each measurement was followed by another with the field reversed, and the appropriate average was formed. In the case of "mixed" second-order terms ($\rho_{23,23}H_2H_3$ for example), the average involved four sign combinations of the field components.

Sample current was set at 10 mA, corresponding to a maximum self-field of 0.0025 G, about 1% of the smallest external fields used, and it was verified that resistance is ohmic for this current and that current reversal produced no new information in all cases.

Experimental plots obtained for a Hall coefficient and for one of the large magnetoresistance terms are shown in Figs. 5 and 6. The size of the applied magnetic fields and the voltages measured may be noted, as well as the small amount of scatter and the deviations from linearity at "high" fields. In contrast, the plots for mixed terms such as $\rho_{23,23}H_2H_3$ usually showed a lot of scatter because of their small size and especially because they are seen only against a background of strong terms.

The deviations from linearity at "high" fields mean that the condition $\mu H/c \ll 1$ is no longer satisfied. For a rough estimate of mobility, one may set $\mu H/c \sim 1/2$ at 2 G, which gives $\mu \sim 2.5\times10^{-7}$ cm²/V-sec, in agreement with Eq. (19) of the following section.

V. RESULTS

Measured values of the galvanomagnetic tensor components at 4.2°K are listed in Table I, together with the results of Abeles and Meiboom[2] at 80° and of Okada[3] at 113°K. The latter have been multiplied by arbitrary factors for comparison with the present data.

Relative sizes of the components $\rho_{ij,kl}$ at 4.2°K are almost identical with those at 80°K and are in fairly good agreement with the 113°K data. According to the

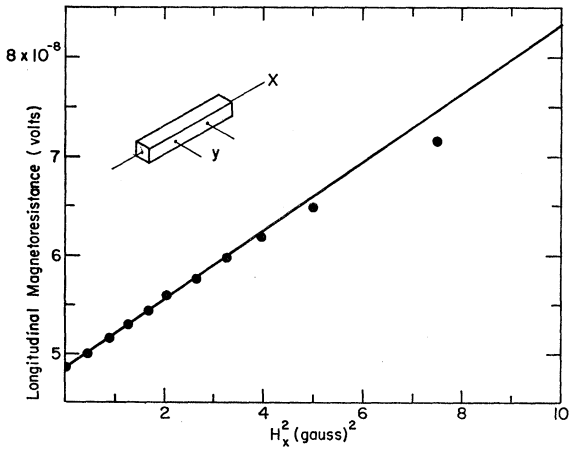

FIG. 6. Experimental plot for the longitudinal magnetoresistance term $\rho_{11,11}$. The sample resistance increases by 30% in a field of only 3 G.

relations (A1) in the Appendix, this is a strong indication that mobilities and carrier concentrations maintain nearly constant proportions over the temperature range.

In contrast, the ratio of the Hall terms $\rho_{ij,k}$ at 4.2°K is quite different than at the other temperatures. Later on it will be clear that a small change in the ratios of electron to hole mobilities has a drastic effect on the value of $\rho_{12,3}$ and only a negligible effect on $\rho_{23,1}$.

Calculations with the data show that $\sigma_{23,23}$ is negative and that Eqs. (10) and (11) are satisfied within the experimental error, so the model outlined earlier may be applied with some confidence.

Analysis of the data by the relations (A1) is a formidable job, and it is reasonable to try to simplify things by assuming, tentatively, that relaxation times are fairly isotropic and that they are not too different for electrons and holes. From known values of effective mass parameters, it follows that μ_2, μ_4, $\nu_3 \ll \mu_1$, μ_3, in which case the relations (A1) reduce to simple forms. Using the abbreviations $x=(eN)^{-1}$ and $y=\mu_1/(\mu_1+2c\nu_1)$, where $c=P/N$, one finds

$$\begin{aligned}
&\rho_{11}{}^0 \doteq 2xy/\mu_1,\\
&\rho_{33}{}^0 \doteq x/\mu_3,\\
&\rho_{23,1} \doteq xy,\\
&\rho_{12,3} \doteq 4xy^2(\mu_1\mu_2 - c\nu_1{}^2)/\mu_1{}^2,\\
&\rho_{11,11} \doteq xy^2\mu_3/2,\\
&\rho_{11,22} \doteq \rho_{11,11} + \text{fairly small terms},\\
&\rho_{11,33} \doteq 4xy^3c\nu_1[(\nu_1/\mu_1)^2 + 4\mu_2\nu_1/\mu_1{}^2 + \mu_2/\mu_1 + \mu_2/2c\nu_1],\\
&\rho_{33,11} \doteq xyc\nu_1,\\
&\rho_{33,33} \doteq x\mu_1(\mu_4/\mu_3)^2,\\
&\rho_{11,23} \doteq xy^2\mu_4,\\
&\rho_{23,11} \doteq xy\mu_4/2,\\
&\rho_{23,23} \doteq -xy^2c\nu_1{}^2/\mu_1.
\end{aligned} \tag{18}$$

These approximations work very well. In the final analysis, of course, the full expressions (A1) must be used, but they alter only by a few percent the results obtained with Eq. (18).

Ratios and other combinations of the above relations give directly many of the unknown quantities, and the selection of a set of unknowns giving the best fit to the data is not difficult. The final, adjusted values are

$$\begin{aligned}
N &= 2.5\times10^{17}\ \text{cm}^{-3} && \pm10\%,\\
c &= P/N = 1.0 && \pm10\%,\\
\mu_1 &= 4.3\times10^{7}\ \text{cm}^2/\text{V sec} && \pm10\%,\\
\mu_2 &= 0.06\times10^{7}\ \text{cm}^2/\text{V sec} && \pm20\%,\\
\mu_3 &= 3.0\times10^{7}\ \text{cm}^2/\text{V sec} && \pm10\%,\\
\mu_4 &= 0.34\times10^{7}\ \text{cm}^2/\text{V sec} && \pm10\%,\\
\nu_1 &= 1.2\times10^{7}\ \text{cm}^2/\text{V sec} && \pm10\%,\\
\nu_3 &= 0.1\times10^{7}\ \text{cm}^2/\text{V sec} && \pm100\%.
\end{aligned} \tag{19}$$

The percentage uncertainties here are not statistically independent. Any one of the quantities may vary within the limits indicated, but usually this requires an adjustment of the values of other quantities, within their limits, in order to conform to the data.

TABLE I. Measured and calculated values of the small field galvanomagnetic tensor components at 4.2°K, in mks units. The $\rho_{ii}{}^0$ are in units of 10^{-9} Ω-m, the $\rho_{ij,k}$ in units of 10^{-5} Ω-m/(Wb/m²) and the $\rho_{ij,kl}$ in units of 10^{-2} Ω-m/(Wb²/m⁴). (1 Wb/m² = 10^4 G.) The data for 80 and 113°K are in arbitrary units for the purpose of comparison; some components were not measured at 80°K.

	4.2°K exp.	4.2°K calc.	80°K Abeles and Meiboom	113°K Okada
$\rho_{11}{}^0$	7.4 ±5%	7.4		
$\rho_{33}{}^0$	8.0	8.1		
$\rho_{23,1}$	1.53±5%	1.52	···	1.5 ±3%
$\rho_{12,3}$	−0.25±8%	−0.26	···	−0.044±10%
$\rho_{11,11}$	1.5 ±10%	1.6	1.6	1.3 ±5%
$\rho_{11,22}$	2.0	1.8	2.4	1.8
$\rho_{11,33}$	0.45	0.42	0.44	0.61
$\rho_{33,11}$	1.9	1.9	1.9	2.3
$\rho_{33,33}$	0.16	0.14	0.16	0.33 ±25%
$\rho_{11,23}$	0.29±15%	0.34	···	0.40
$\rho_{23,11}$	0.20	0.26	···	0.19 ±30%
$\rho_{23,23}$	−0.33±20%	−0.36	···	−0.15 ±40%

Resistivity components calculated from Eq. (19) are listed in Table I; agreement with the data is satisfactory. The large uncertainties in the values of μ_2 and particularly μ_3 are unavoidable because they make relatively small contributions to the observed components.

The electron ellipsoid tilt angle, given by Eq. (9), is 6.5°, which compares favorably with the value 5.8° from Aubrey's cyclotron resonance work.[15] This agreement supports the validity of the present theoretical analysis, particularly the Herring-Vogt approximation of isotropic relaxation time components.

Relaxation times are obtained from a comparison of the diagonalized mobility and reciprocal effective mass tensors. The mass parameters of Galt *et al.*[16] and of Aubrey give the following components (in the ellipsoid axes frame) for electrons:

$$\begin{aligned}
\tau_1 &= 2.2(1.2)\times10^{-10}\ \text{sec},\\
\tau_2 &= 1.9(1.2)\times10^{-10}\ \text{sec},\\
\tau_3 &= 1.6(2.1)\times10^{-10}\ \text{sec}.
\end{aligned} \tag{20}$$

The numbers in parentheses come from Aubrey's masses. For holes, Galt's data give

$$\begin{aligned}
\tau_1 &= 4.3\times10^{-10}\ \text{sec},\\
\tau_3 &\doteq 5\ \times10^{-10}\ \text{sec}.
\end{aligned} \tag{21}$$

It can be concluded that electron and hole relaxation times are isotropic to within a factor of 2 and that hole relaxation times are larger than those for electrons by a factor of 2 or 3. The values agree with Galt's estimates from cyclotron resonance. In an unpublished work per-

[15] J. E. Aubrey, thesis, Cambridge University, 1958 (unpublished).

[16] J. K. Galt, W. A. Yager, F. R. Merritt, B. B. Cetlin, and A. D. Brailsford, Phys. Rev. **114**, 1396 (1959).

formed at this laboratory, Mase obtained relaxation times at 20.4°K from high-field galvanomagnetic measurements which are in the same relative proportions as those of Eqs. (20) and (21) but are smaller by a factor of 6.

The relatively small anisotropy in Eqs. (20) and (21) is encouraging; as discussed in a previous section, the validity of the Herring-Vogt model would be doubtful if the anisotropy were larger.

Turning now to the carrier concentrations, one calculates the electron concentration per ellipsoid as 0.91×10^{17} cm^{-3} from Aubrey's masses and Shoenberg's value of 0.0177 eV for the Fermi energy. Weiner[17] has applied a correction for nonparabolic energy bands and obtains 0.95×10^{17} cm^{-3} for the concentration per ellipsoid. The total concentration found in the present experiment is $2.5\times10^{17}\pm10\%$, so the conduction band must consist of three ellipsoids.

It must be emphasized at this point that an interpretation of the present data consistent with six ellipsoids, i.e., a total concentration of about 5×10^{17} cm^{-3}, is strictly impossible. A direct proof of this contention rests on the value of the Hall coefficient $\rho_{23,1}$. Besides being one of the most accurately determined components (see Fig. 5), it is actually measured three ways on the two different samples, as indicated by Eqs. (13), (14), and (17), and the results agree within 5%. Now, inspection of the exact expression for $\rho_{23,1}$ given in the Appendix shows that the entire quantity to the right of the term $(1/eN)$ must always be less than unity. It follows that N is bounded:

$$N<1/(e\rho_{23,1})=4.1\times10^{17}\text{ cm}^{-3}. \tag{22}$$

A necessary condition for N to approach its upper bound is $2c\nu_1\ll\mu_1$, but this is entirely incompatible with the values of at least two other accurately determined components, namely, the zero-field resistivity ρ_{11}^0 and the transverse magnetoresistance coefficient $\rho_{33,11}$. The conditions $2c\nu_1\ll\mu_1$ and $N\doteq1/e\rho_{23,1}$ lead to a self-contradiction: One gets the values $\mu_1\doteq4\times10^7$ cm^2/V-sec (from ρ_{11}^0) and $c\nu_1=1.2\times10^7$ cm^2/V-sec (from $\rho_{33,11}$). To put it another way, the hole mobility term $c\nu_1$ is known to be comparable with electron mobilities simply because the magnetoresistance coefficient depending almost entirely on this hole term is, in fact, one of the largest of the $\rho_{ij,kl}$ components.

Accordingly, N must be somewhat less than the right side of (22) and therefore much smaller than the value of 5×10^{17} cm^{-3} required for the six-ellipsoid model.

It may be argued that the sample happens to contain just the concentration of acceptor impurities necessary to lower N to half the value for pure bismuth. This is quite unlikely, because in such an event the lowered Fermi level requires a value of $c=P/N$ which is certainly greater than 2 (even if a heavy-hole band exists). In this case, a fit of the data is not possible unless one or more of the tensor components has been incorrectly measured by factors of 3 and more.

The value of c deduced in the present experiment happens to be fairly precise because it has a strong effect in the components $\rho_{12,3}$ and $\rho_{11,33}$, and in attempting to vary c, the product $c\nu_1$ must be kept nearly constant, as required by the ratio $\rho_{33,11}/\rho_{23,1}$ from Eq. (18).

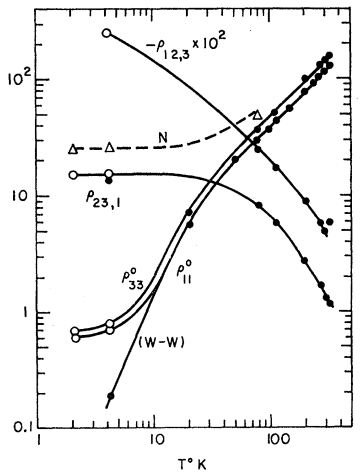

FIG. 7. Zero-field resistivities, Hall coefficients, and carrier concentration in various units as a function of temperature. The sources of the data assembled here are described in the text.

The result $c=1.0\pm0.1$ leaves no room for a heavy-hole band. Also, it seems that there is just one light-hole ellipsoid; from the carrier concentration and Galt's masses for holes, the Fermi energy is calculated as 9.5×10^{-3} eV, which may be compared with the value 11×10^{-3} eV obtained by combining Brandt's[18] de Haas-van Alphen measurements of Fermi momenta with Galt's masses.

Size effects in the experiment are small. The longest mean free path is 0.18 mm, compared to the sample thickness of 8 mm. Calculations[4,19] indicate that only a 3% correction should be added to N for the true bulk value, and this is consistent with experimental results obtained after thinning the sample slightly.

VI. TEMPERATURE EFFECTS

Data from a number of sources have been gathered in Fig. 7, showing the over-all temperature dependence of zero-field resistivities and small-field Hall coefficients. At 80°K and above, the information comes mainly from Okada[3] and Abeles and Meiboom.[2] White and Woods[20] measured "zero-field" resistivities of polycrystalline samples over the entire temperature range and, by subtracting residual resistivities, obtained the "ideal" curve in the figure labeled "W-W." The points at 20°K were obtained by Mase at this laboratory. Open circles in the figure at 4.2 and 2.1°K are the result of the present experiment; the dark circles at 4.2° are approximate

[17] D. Weiner, Bull. Am. Phys. Soc. **6**, 439 (1961).

[18] N. V. Brandt, Soviet Phys.—JETP **11**, 975 (1960).

[19] P. J. Price, IBM J. Research Develop. **4**, 152 (1960).

[20] G. K. White and S. B. Woods, Phil. Mag. **3**, 341 (1958).

and represent extrapolated bulk values deduced from the size-effect data of Friedman and Koenig[4] for one of their samples. Its resistivity indicates a high degree of purity and crystal perfection.

Figure 7 also includes a curve at low temperatures for the carrier concentration N, assuming three ellipsoids, a Fermi energy of 0.018 eV, and a mean density of states mass $m^*=0.042m_0$ from Aubrey's cyclotron resonance data. (At temperatures of 100°K and above, N will receive increasing contributions of thermally excited carriers from other bands.) Triangular points indicate the values of N found by the present author at helium temperature and by Abeles and Meiboom at 80°K.

The figure illustrates nicely some points discussed in the previous section. From the correspondence of $\rho_{ij,kl}$ data in Table I, it was concluded that all mobilities change nearly the same way with temperature. Therefore, according to Eq. (18), the Hall term $\rho_{23,1}$ is proportional to N^{-1} and some factor which is insensitive to temperature. However, $\rho_{12,3}$ depends on the difference of ν_1^2 and $\mu_1\mu_2$. These are nearly equal at 80°K and above, so a slight change in the proportions of mobilities at lower temperatures has a large effect. The figure, in fact, illustrates what happens when mobility ratios change by only 30% from 80 to 4.2°K. The effect may be gradual over this temperature range, or it might occur only when the scattering processes of the residual resistance region are encountered. A measurement of $\rho_{12,3}$ at intermediate temperatures or in various samples at 4.2°K would clarify this point.

The resistivity curves merit attention. If the "ideal" curve of White and Woods is taken seriously, one obtains the interesting result shown in Fig. 8, namely, a mobility varying as reciprocal temperature squared. For a simple metal, the usual Grüneisen–Bloch relation predicts a T^{-5} dependence at low temperatures, as observed in sodium and some other monovalent metals. Careful measurements on large monocrystals of high-purity bismuth need to be made to verify the White and Woods result which, if true, poses an interesting theoretical problem and may provide clues to the scattering process at low temperatures.

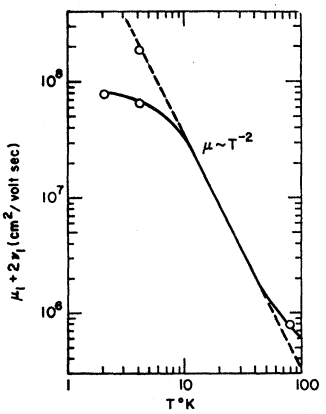

FIG. 8. Mobility vs temperature. This curve is derived from values of the carrier concentration and the "ideal" resistivity curve of White and Woods shown in Fig. 7.

VII. "LARGE" MAGNETIC FIELDS

In some instances during the experiment, galvanomagnetic effects were studied at fields larger than usual and with a curious effect. With increasing fields, the magnetoresistance enters a region in which it varies with field to the power 1.6. On a log-log graph, the plot is "perfectly" straight. The range usually extended from about 3 to 50 G, the latter being the largest available with the equipment. Essentially the same phenomenon in the kilogauss range is seen in the data of Mase and Tanuma[21] at 4.2°K and also in the unpublished work of Mase at 20.4°K performed at this laboratory.

No theoretical explanation seems to be available. The effect conceivably might be geometric, i.e., the result of an insufficient length-to-width ratio for the case of very large Hall angles. Further investigation was not possible at the time of this writing.

VIII. CONCLUSIONS

From small-field galvanomagnetic measurements at 4.2°K, it is concluded that the electron concentration is 2.5×10^{17} cm^{-3}, and the concentration of "light" holes is very nearly the same. When compared with cyclotron resonance and de Haas-van Alphen experiments, the results are consistent with a three-ellipsoid model for electrons and a single ellipsoid for "light" holes. There is no indication of the presence of "heavy" holes in a concentration comparable to the other carriers.

The theory used to interpret the data certainly can be criticized on the grounds that the transport process is not analyzed exactly; instead, a number of simplifying assumptions are made, e.g., the existence of a relaxation time tensor with isotropic components. Although this procedure has worked fairly well in the past for other solids, there is no guarantee that the method is valid for bismuth. Nevertheless, the analysis does show a number of internal consistencies, such as the agreement of the ellipsoid tilt angle value with cyclotron resonance data, and the relatively small differences in the components of τ.

The discrepancies between various experimental investigations of ellipsoid multiplicities and of heavy holes are certainly unresolved; in fact, the oscillatory magnetoresistance measurements made by Lerner[22] of this laboratory indicate the presence of a heavy carrier with isotropic mass. It may be that a band model more complicated than the ones usually proposed can explain the variety of experimental results in bismuth.

ACKNOWLEDGMENTS

The author is grateful to members of his doctoral committee—Professor A. W. Lawson, Professor M. H. Cohen, and Professor H. Fritzsche—for their advice and for many enlightening conversations.

[21] S. Mase and S. Tanuma, J. Phys. Soc. Japan **14**, 1644 (1959).
[22] L. S. Lerner, following paper [Phys. Rev. **127**, 1480 (1962)].

APPENDIX

$$\rho_{11}^{0}=(2/eN)(\mu_1+\mu_2+2c\nu_1)^{-1},$$

$$\rho_{33}^{0}=(1/eN)(\mu_3+c\nu_3)^{-1},$$

$$\rho_{23,1}=(1/eN)[(\mu_1+\mu_2)\mu_3-\mu_4^2-2c\nu_1\nu_3]\times(\mu_1+\mu_2+2c\nu_1)^{-1}(\mu_3+c\nu_3)^{-1},$$

$$\rho_{12,3}=(4/eN)(\mu_1\mu_2-c\nu_1^2)(\mu_1+\mu_2+2c\nu_1)^{-2},$$

$$\rho_{11,11}=(1/2eN)[(\mu_1-\mu_2)^2\mu_3+(5\mu_1-\mu_2)\mu_4^2]\times(\mu_1+\mu_2+2c\nu_1)^{-2},$$

$$\rho_{11,22}=(1/2eN)(\mu_1+\mu_2+2c\nu_1)^{-2}\{3\mu_1^2\mu_3+(2\mu_1+3\mu_2)(\mu_2\mu_3-\mu_4^2)+\mu_1\mu_4^2+8c\nu_1^2\nu_3-[(\mu_1+\mu_2)\mu_3-\mu_4^2-2c\nu_1\nu_3]^2(\mu_3+c\nu_3)^{-1}\},$$

$$\rho_{11,33}=(2/eN)(\mu_1+\mu_2+2c\nu_1)^{-2}[\mu_1\mu_2(\mu_1+\mu_2)+2c\nu_1^3-4(\mu_1\mu_2-c\nu_1^2)^2(\mu_1+\mu_2+2c\nu_1)^{-1}],$$

$$\rho_{33,11}=(1/2eN)(\mu_1+\mu_2+2c\nu_1)^{-1}(\mu_3+c\nu_3)^{-2}\times\{2(\mu_1+\mu_2)(\mu_3+c\nu_3)^2c\nu_1+\mu_4^2[(\mu_1-\mu_2)\mu_3-\mu_4^2+4c\nu_1(2\nu_3-\mu_3)]\},$$

$$\rho_{33,33}=(1/eN)\mu_1\mu_4^2(\mu_3+c\nu_3)^{-2},$$

$$\rho_{11,23}=(1/eN)\mu_1\mu_4(\mu_1-\mu_2)(\mu_1+\mu_2+2c\nu_1)^{-2},$$

$$\rho_{23,11}=(1/2eN)[(\mu_1-\mu_2)\mu_3\mu_4+\mu_4^3]\times(\mu_1+\mu_2+2c\nu_1)^{-1}(\mu_3+c\nu_3)^{-1},$$

$$\rho_{23,23}=-(1/eN)(\mu_1+\mu_2+2c\nu_1)^{-2}(\mu_3+c\nu_1)^{-1}\times\{\mu_1\mu_2\mu_4^2+2\mu_1\mu_2c\nu_1(\mu_3+c\nu_3)+c\nu_1^2[(\mu_1+\mu_2)\mu_3-\mu_4^2-2c\nu_1\nu_3]\}. \quad \text{(A1)}$$

PHYSICAL REVIEW VOLUME 127, NUMBER 5 SEPTEMBER 1, 1962

Shubnikov-de Haas Effect in Bismuth*†

LAWRENCE S. LERNER‡
Department of Physics and Institute for the Study of Metals, University of Chicago, Chicago, Illinois

(Received April 4, 1962)

The oscillatory component of the transverse magnetoresistance of bismuth has been measured as a function of magnetic field orientation at liquid helium temperatures. A derivative technique was employed. In addition to sets of periods, observed in the de Haas-van Alphen effect by Shoenberg and by Brandt and attributed by them, respectively, to the electron and light-hole Fermi surfaces, we observe a new set of isotropic short periods, $P=0.72\times10^{-5}$ G^{-1}. The squares of the electron Fermi momenta $m_0\kappa_{11}^2$, $m_0\kappa_{22}^2$, $m_0\kappa_{33}^2$, $m_0\kappa_{23}^2$ are, respectively, 0.189, 45.4, 0.918, and -4.54 m_0 milli-electron volts (meV). For the light holes, $m_0\kappa_{11}^2$ and $m_0\kappa_{33}^2$ are 1.51 and 21.0 m_0 meV. For the new heavy carriers, $m_0\kappa^2=3.18$ m_0 meV. These data are fitted to two possible three-carrier models of the Fermi surface, and to a four-carrier model. Significant deviations of the oscillations from periodicity in H^{-1} are observed for the electron part of the Fermi surface for certain magnetic field orientations.

I. INTRODUCTION

THE Fermi surface of the semimetal bismuth has been extensively investigated by means of the de Haas-van Alphen effect[1–6] and other measurements based upon the same quantization condition,[7–16] by means of cyclotron resonance[17–22] and surface resistance measurements,[23,24] and by means of the galvanomagnetic effects.[25–31] In general, the experimental results

* Submitted as a thesis in partial fulfillment of the requirements for the degree of Doctor of Philosophy at the University of Chicago.

† This work was supported in part by a grant from the National Science Foundation.

‡ Now at Hughes Research Laboratories, Malibu, California.

[1] D. Shoenberg and M. Z. Uddin, Proc. Roy. Soc. (London) **A156**, 687 (1936).
[2] D. Shoenberg, Proc. Roy. Soc. (London) **A170**, 341 (1939).
[3] J. S. Dhillon and D. Shoenberg, Phil. Trans. Roy. Soc. London **A248**, 1 (1955).
[4] D. Weiner, Phys. Rev. **125**, 1226 (1962).
[5] N. B. Brandt, A. E. Dubrovskaia, and G. A. Kytin, Soviet Phys.—JETP **10**, 405 (1960).
[6] N. B. Brandt, Soviet Phys.—JETP **11**, 975 (1960).
[7] W. C. Overton and T. G. Berlincourt, Phys. Rev. **99**, 1165 (1955).
[8] J. Babiskin, Phys. Rev. **107**, 981 (1957).
[9] J. M. Reynolds, H. W. Hemstreet, T. E. Leinhardt, and D. D. Triantos, Phys. Rev. **96**, 1203 (1954).
[10] P. B. Alers and R. T. Webber, Phys. Rev. **91**, 1060 (1953).
[11] R. A. Connell and J. A. Marcus, Phys. Rev. **107**, 940 (1957).
[12] D. H. Reneker, Phys. Rev. **115**, 303 (1959).
[13] W. S. Boyle, F. S. L. Hsu, and J. E. Kunzler, Phys. Rev. Letters **4**, 278 (1960).
[14] W. S. Boyle and K. F. Rodgers, Phys. Rev. Letters **2**, 338 (1959).
[15] M. C. Steele and J. Babiskin, Phys. Rev. **98**, 359 (1955).
[16] Y. Eckstein and J. Ketterson (private communication).
[17] J. E. Aubrey and R. G. Chambers, J. Phys. Chem. Solids **3**, 128 (1957).
[18] J. E. Aubrey, thesis, Cambridge University, 1958 (unpublished).
[19] J. K. Galt, W. A. Yager, F. R. Merritt, B. B. Cetlin, and H. W. Dail, Phys. Rev. **100**, 748 (1955).
[20] J. K. Galt, W. A. Yager, F. R. Merritt, B. B. Cetlin, and A. D. Brailsford, Phys. Rev. **114**, 1396 (1959).
[21] R. N. Dexter and B. Lax, Phys. Rev. **100**, 1216 (1955).
[22] Y. H. Kao, J. I. Budnick, and S. H. Koenig, Bull. Am. Phys. Soc. **6**, 439 (1961).
[23] G. E. Smith, Phys. Rev. **115**, 1561 (1959).
[24] G. E. Everett (to be published).
[25] B. Abeles and S. Meiboom, Phys. Rev. **101**, 544 (1956).
[26] A. L. Jain, Phys. Rev. **114**, 1518 (1959).
[27] R. N. Zitter, preceding paper [Phys. Rev. **127**, 1471 (1962)].